Ann. Naturhist. Mus. Wien	106 A	259–279	Wien, November 2004

The Cretaceous-Paleogene boundary section of Gorgo a Cerbara: an integrated stratigraphical study

by Christine LATAL[1]

(With 8 text-figures and 2 tables)

Manuscript submitted on 20 December 2003,
the revised manuscript on 11 May 2004

Abstract

An integrated stratigraphical study has been performed at the Cretaceous-Paleogene transition section of Gorgo a Cerbara in North Umbria (Italy). A magnetostratigraphy for the section was established which was correlated to biostratigraphy with calcareous nannofossils and stable isotope stratigraphy. The nearly 30 m long section of Cerbara is built up of typical Scaglia Rossa limestones and marly limestones. Magnetostratigraphic results for the Cerbara section, and particularly the Cretaceous part, correlate well with the nearby Gubbio section. Magnetozones 31N to 26R were identified in the Cerbara section. Biostratigraphy with calcareous nannofossils did not yield results with a high resolution because of recrystallisation and dissolution effects on the fossils. In the Cretaceous, nannoplankton zones NC22 and NC23 (ROTH 1978) were identified by the occurrence of *Lithraphidites quadratus* and *Micula murus*. Although typical Paleogene forms like *Thoracosphaera operculata, Braarudosphaera bigelowii, Coccolithus pelagicus* and *Chiasmolithus danicus* were recognized above the boundary, no evident nannoplankton zonation could be established. The section probably ends in nannozone NP4 (MARTINI 1971). Values of oxygen and carbon isotopes indicate a diagenetic overprint. Nevertheless, a drastic decrease of $\delta^{13}C$ directly above the Cretaceous-Paleogene boundary was determined, as well as an increase in $\delta^{18}O$.

1. Introduction

The mass extinction event at the Cretaceous-Paleogene (C/P) boundary is one of the most discussed matter in geosciences and the best studied mass extinction event in the geological record (GARDIN 2002). Although five major mass extinction events are known from the Phanerozoic (RAMPINO & HAGGERTY 1996, MACLEOD 1996), the C/P boundary has aroused the highest attention because of the hypothesis that an asteroid may have hit the Earth at the end of the Cretaceous and caused the mass extinction (ALVAREZ et al. 1980). Since this time many controversies on this matter seem to have been solved, e. g. the impact at or near the boundary at Chicxulub, Yucatan Peninsula in Mexico (HILDEBRANDT et al. 1991, POPE et al. 1991, KYTE 1998) exists, but debates on the effects of this impact and the nature of the mass extinction are still going on. Thus, the literature on the C/P boundary is immense. The hypothesis of ALVAREZ et al. (1980) is based on the high iridium content of the boundary clay in the nowadays famous section of Gubbio in the Umbria-Marche region (Italy). Throughout this region numerous C/P boundary sections are exposed and many of them have been studied to some extent (ALVAREZ & LOWRIE 1984, CHAN et al. 1985, MONTANARI & KOEBERL 2000).

[1] Mag. Dr. Christine LATAL, Institute for Earth Sciences, University of Graz, Heinrichstraße 26, A-8010 Graz, Austria. – e-mail: christine.latal@uni-graz.at

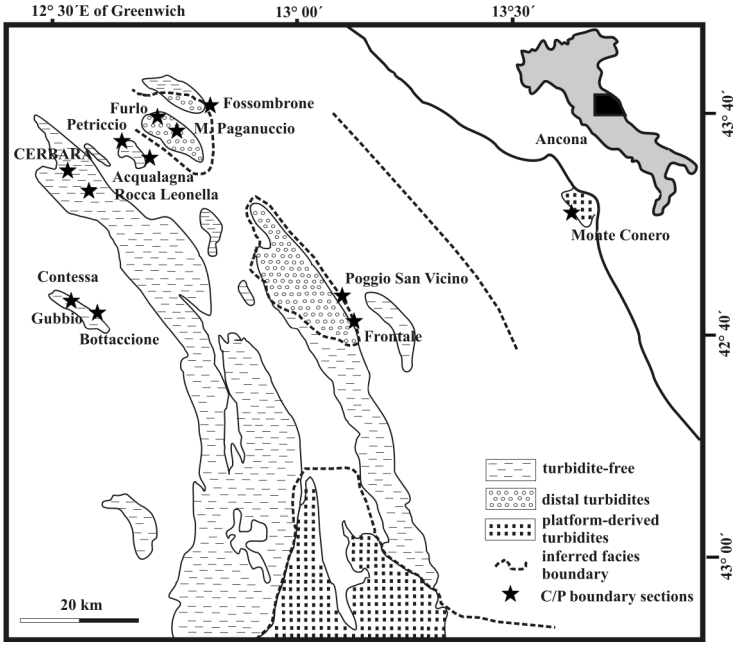

Fig. 1: Facies map of the Scaglia Rossa formation in the northeastern Apennines with locations of C/P boundary sections (after MONTANARI 1991)

For the boundary clay in the Cretaceous-Paleogene section at Gorgo a Cerbara the iridium anomaly is proved (MONTANARI 1991), but other stratigraphical data are missing. Therefore this section was investigated in a combined magneto-, bio- and isotope stratigraphical study.

The Scaglia Rossa Formation in the Umbrian Marche Sequence in Italy has been studied very intensively in the last decades for sedimentological settings, tectonic evolution (ARTHUR & FISCHER 1977, BALDANZA et al. 1982, ALVAREZ et al. 1985, MONTANARI et al. 1989, MONTANARI & KOEBERL 2000), calcareous plankton biostratigraphy (LUTERBACHER & PREMOLI SILVA 1962, PREMOLI SILVA 1977, MONECHI 1977, MONECHI & THIERSTEIN 1985, PREMOLI SILVA & SLITER 1995), magnetostratigraphy (ALVAREZ et al. 1977, ROGGENTHEN & NAPOLEONE 1977, LOWRIE & ALVAREZ 1977, 1981, LOWRIE et al. 1982, ALVAREZ & LOWRIE 1978, 1984, CHAN et al. 1985) and stable isotope chemostratigraphy (CORFIELD et al. 1991).

But poor preservation of nannoplankton (MONECHI & RADRIZZANI 1975, MONECHI 1977, MONECHI & THIERSTEIN 1985) in this area is still a limiting factor for a good correlation of nannofossils with the global polarity time scale (GPTS).

At the C/P boundary, about 90% of the Cretaceous calcareous nannoplankton species became extinct. In connection with the debate, whether the mass extinction was suddenly or not, it is interesting that there is no hint in the fossil nannoplankton record of a gradual extinction. The upper Maastrichtian nannoplankton community was essentially stable until the C/P boundary (GARDIN 2002). In the earliest Paleogene sediments usually true survivor taxa, dominated by *Thoracosphaera* and *Braarudosphaera*, are found, followed shortly by an interval dominated by very small (< 3µm) incoming species, like *Biscutum romeinii, Biscutum parvulum, Cruciplacolithus primus, Prinsius dimorphosus*, and *Toweius petalosus* (GARTNER 1996).

Stable isotopes studies at the Cretaceous-Paleogene boundary have been performed worldwide. One of the best studied sections is the boundary-stratotype (GSSP) at El Kef in Tunisia (KELLER & LINDINGER 1989, REMANE &ADATTE 2002). A negative $\delta^{13}C$ shift in fine fraction carbonate, reduced $CaCO_3$ accumulation, and faunal changes have been observed in every C/P boundary sequence examined globally (THIERSTEIN & BERGER 1978, SCHOLLE & ARTHUR 1980, PERCH-NIELSEN et al. 1982, ZACHOS & ARTHUR 1986, ARTHUR et al. 1987, STÜBEN et al. 2002). The global decrease in $\delta^{13}C$ of surface water is generally interpreted as resulting from a sudden reduction of oceanic primary productivity (THIERSTEIN & BERGER 1978, HSÜ et al. 1982, PERCH-NIELSEN et al. 1982, ARTHUR et al. 1987), because the $\delta^{13}C$ distribution in the oceans is largely controlled by primary productivity in surface waters, and organic carbon oxidation and CO_2 regeneration in deep waters (WILLIAMS et al. 1977, KROOPNICK 1980). In contrast to this uniform carbon isotope signal, $\delta^{18}O$ values show globally contradicting trends.

2. Regional Geology

The Apennine, located in the Umbria-Marche region of Italy, is an unmetamorphosed foreland fold and thrust belt, formed during the latest phase of the Alpine-Himalaya orogenesis. The tectonic history of the Northern Apennine mountain belt is very complex: the sedimentary sequence comprises the evolution from an Early Jurassic to Paleogene carbonate sequence to a synorogenic and post-orogenic siliciclastic sequence deposited in the Neogene and Quaternary (MONTANARI & KOEBERL 2000). In Late Triassic to Early Jurassic time rifting between Europe and Africa formed a new oceanic basin which traces the rough outline of a northward-pointing promontory of the African continental crust, the so called Adria or the Adriatic Promontory (CHANNEL et al. 1979). The Adriatic Promontory was isolated from the input of clastic sediments (MONTANARI & KOEBERL 2000).

The section of Gorgo a Cerbara (43.6°N; 12.56°E) is made of the typical pelagic limestones of the Scaglia Rossa Formation (Upper Cretaceous-Eocene).

The Scaglia Rossa Formation is a coccolith-foraminiferal deepwater pelagic limestone and shows three sedimentary facies (MONTANARI 1991) (Fig. 1): the proximal turbiditic facies is characterised by platform derived calcareous turbidites, interbedded with biomicritic pelagic limestones. Characteristics of the distal turbiditic facies are very fine calcarenitic turbidites, which were trapped in intrabasinal depocenters, and are interbedded with biomicritic pelagic limestones. The turbidite free facies consists of pelagic limestones and marls.

The Scaglia Rossa Formation is divided into 4 members (MONTANARI et al. 1989). The R1 member (Turonian to Lower Campanian) consists of pink and white limestones containing nodular cherts. The chert free members R2 and R3 consist of limestones and marls. In areas with proximal facies, chert nodules can be found within the calcareous turbidites in the R2 member (Upper Campanian to Maastrichtian) and therefore the distinction between this member and the underlying R1 is difficult. The R3 member (Danian to Lower Ypresian) ranges from the first appearance of nodular chert at the top to the Cretaceous-Paleogene boundary at the bottom. The R4 member (Ypresian to Lower Lutetian) consists of white and pink marls and limestones containing nodular cherts.

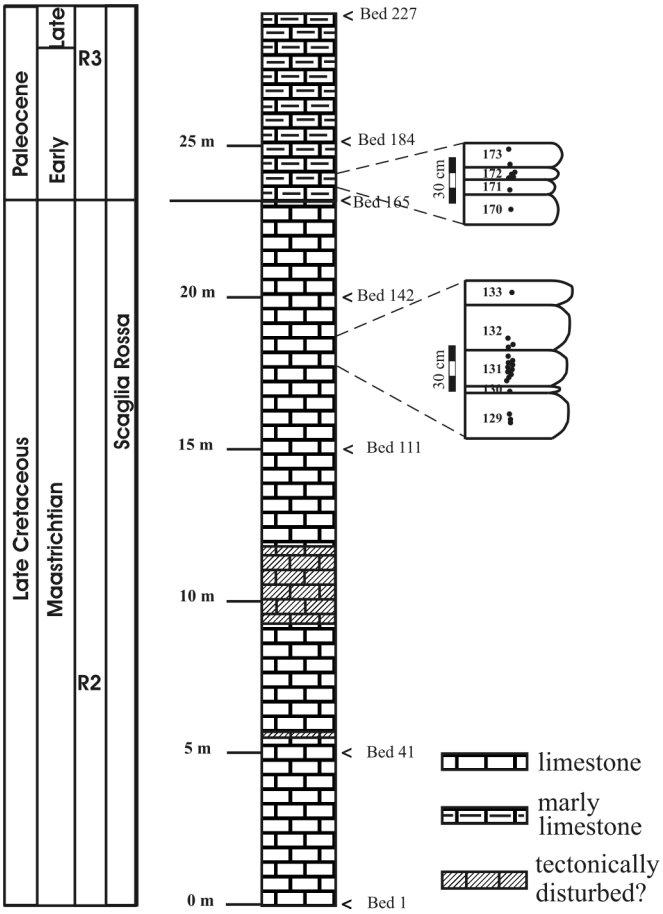

Fig. 2: Schematic stratigraphy of the Scaglia Rossa sequence and lithological profile of the Cerbara section; enlarged details show examples of sampling density.

The nearly 30 m long section of Cerbara (Fig. 2), built up of parts of the R2 member in the Maastrichtian and R3 in the Paleocene, is bounded on both sides by big faults. The Cretaceous part is about 23.5 m and the Paleogene about 6 m long. The section is built up of micritic pink and sometimes white pelagic limestones, and marly limestones with mm-thin shale interbeds. Bed thickness of the limestone varies between 5 cm and 30 cm, and bedding-planes are well defined.

In the Cretaceous planktonic foraminifera are dominated by assemblages of large *Globotruncana*, while in the Paleogene small forms of *Globigerina* are found. Within the Paleogene part of the section planktonic foraminifera rise in size and number from the C/P boundary to the top.

Large parts of the section are not influenced by tectonics, but at 5.5 m (bed 45) a small fault is observable. The range between 9.0 m and 11.8 m (bed 78 to 95) could have been affected by a synsedimentary sliding. The Cretaceous part from 14.2 m (bed 107) up to the Cretaceous-Paleogene boundary is certainly undisturbed.

Styloliths, indicating pressure solution during compaction, and bioturbation occur in the Cretaceous as well as in the Paleogene part of the section. The weathering of the limestones is quite weak. The Cretaceous-Paleogene boundary is represented by a 2.5 cm thick green and red clay layer (bed 165) at 23.2 m.

3. Sampling and Methods

Each of the 206 consecutively numbered limestone beds of the section has been sampled, and at least one oriented core for paleomagnetic investigations was taken. The cores of 2.5 cm diameter were collected by using a portable coring apparatus with a non-magnetic hollow drill bit. The average sample density was one every 15 cm. The oriented cores were cut into standard specimens, 2.2 cm long, and then used for the paleomagnetic laboratory analyses in the Paleomagnetic Laboratory in Gams, University of Leoben. Natural remanent magnetization (NRM) was measured on a three-axes cryogenic magnetometer with an in-line degausser (2G Enterprises). Geofyzika KLY-2 was used for measuring low-field magnetic susceptibility and its anisotropy. The magnetic mineralogy was studied by coercivity spectrum analyses (LOWRIE 1990), three-component isothermal remanent magnetization (maximum field of 1.5 Tesla) and thermal demagnetization of IRM.

Specimens not used for paleomagnetic investigations or remainders of the drilled cores were used for thin-sections and for getting powder for smear slides and the analyses of stable isotopes. For smear slides and stable isotope investigations in the Cretaceous a sample density of about 1 m was selected. Across the C/P boundary from 22.0 m to 24.4 m smear slides and isotope analyses were made from every limestone bed (156-176). In the Paleogene every 30-50 cm samples were chosen for investigations on calcareous nannofossils and stable isotopes. For isotope analyses a small drilling machine was used to get powder of about 0.1-0.2 mg from the core samples. Carbonate powder was reacted with 100% phosphoric acid at 70°C in a Finnigan Kiel II automated reaction system and measured with a Finnigan Delta Plus isotope-ratio mass spectrometer at the Institute of Geology and Palaeontology, University of Graz. Values are given against VPDB. The laboratory precision for $\delta^{18}O$ and $\delta^{13}C$ is better than 0.1 ‰.

4. Results

4.1. Magnetic results

Natural remanent magnetization intensities vary between 0.17×10^{-3} and 17×10^{-3} A/m (normalized to sample mass) and the susceptibility data range from 0.156×10^{-6} to 6.26×10^{-6} SI. Declination and inclination data indicate the occurrence of both polarities.

The magnetic mineralogy was studied by isothermal remanent magnetization analyses. Fields of up to 1450 mT and a backfield up to 300 mT were applied. The samples show relatively homogeneous properties: Progressively increasing magnetizing fields up to 1.45 T produced isothermal remanence curves with steep gradients up to 0.2 T, charac-

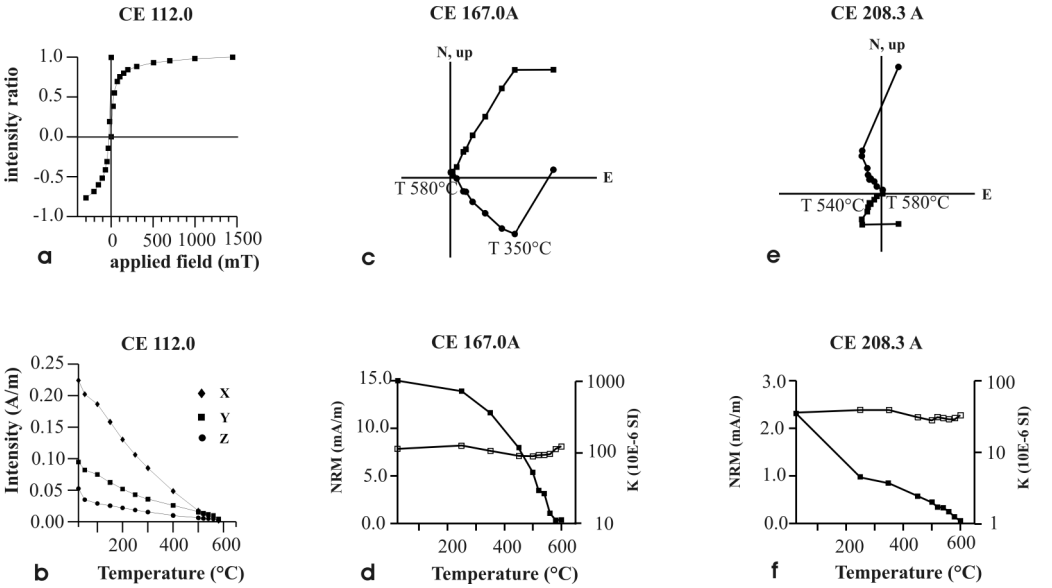

Fig. 3: Magnetic characteristics of the Scaglia Rossa limestones: a) IRM acquisition curve; b) thermal demagnetization of IRM with different fields in 3 orthogonal directions (x = 0.1 T; y = 0.5 T; z = 1.45 T); c) and e) Zijderveld diagrams (circles show the horizontal component, squares the vertical component) of representative samples with reversed (CE 167.0A) and normal polarity (CE 208.3A); d) and f) decrease of magnetization intensity (filled squares) and properties of magnetic susceptibilty (open squares) during thermal treatment.

teristic for magnetite as the dominant magnetic mineral. In all samples saturation was not reached until 1.45 T, indicating the presence of an additional high coercivity component (goethite or hematite) (Fig. 3a) (SOFFEL 1991). Furthermore, the samples were subjected to different magnetizing fields in 3 orthogonal directions (z: 1.45 T; y: 0.5 T; x: 0.1 T) and then thermally demagnetised (Fig 3b). The hard component shows a clear drop below 100°C in most of the samples. This drop, in connection with the presence of a high coercivity component, allowed to identify goethite as a magnetic component. The medium and hard coercivity components have vanished at 250°C. The soft component demagnetised straight to zero in the temperature range 570-590°C. From the coercivity spectrum analyses it is concluded that samples are dominated by magnetite with small amounts of goethite and hematite.

Thermal treatment led to a successful demagnetization of most of the samples and revealed the presence of multicomponent magnetization in the specimens (Fig. 3c, e). One component, probably a viscous remanent magnetization (VRM), was removed at 250°C and is in alignment with the present geomagnetic dipole field. The characteristic remanent magnetization vector (ChRM) was defined above 350°C in some samples, in others only above 540°C. In both cases the ChRM was carried by magnetite. In some samples another component (carried by hematite) persisted after heating above 580°C with remanence direction parallel to the direction of the magnetite component. Magnetic susceptibility

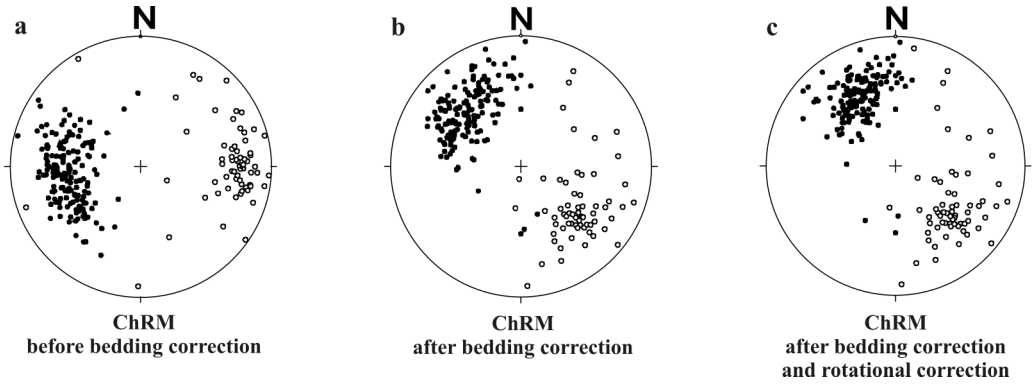

Fig. 4: Stereoplots of ChRM directions before bedding correction, after bedding correction and after bedding and rotational correction (open circles indicate negative inclination, filled circles positive inclination).

showed no increase during heating up to 600°C (Fig 3d, f). The ChRM vectors carried by magnetite, and in some cases also by hematite, show both polarities. Before bedding correction the direction of declination for normal polarity data is W, for reversed polarity data E with inclinations of about 35° and –25° (Fig. 4a). After bedding correction these directions rotate to NW and SE respectively (Fig. 4b). The declination directions of the ChRM of the normal polarity showed a good statistical fit, nevertheless they scattered quite largely between W and NW. When the declination data were plotted against their stratigraphical position, this scatter turned out to be a regular rotation. Samples of the lower part of the section showed W-directions of the declination, while samples of the upper part showed NW-directions. Measurement of the magnetic anisotropy verified this feature (LATAL et al. 2000).

The measured anisotropy of the low-field magnetic susceptibility indicated a primary sedimentary origin of the magnetic fabric with an oblate shaped susceptibility ellipsoid. The maximum susceptibility axes (98 statistically significant data) were aligned within the bedding plane while the minimum susceptibility axes, with 159 statistically significant data, were aligned perpendicular to the bedding plane and reflected the poles to the bedding plane. The K_{min} axes of the data set indicate a rotation, and the same trend was obvious in the K_{max} axes as well as in the ChRM declination. Three homogenous zones in the section were separated. Boundaries between these zones are represented by small steep faults. The angle between the first and the third zone indicated a rotation of about 30° under the assumption that the rotation was around an axis perpendicular to the bedding plane. To take into account a different type of tectonic deformation, a fold axis of an inclined fold was calculated from the bedding planes. For both types of deformation, fold axis and rotation perpendicular to the bedding plane, corrections have been made (Tab. 1). For magnetostratigraphy ChRM data after bedding correction and additional rotational correction are used although these corrections do not influence the polarity sequence within the section (Fig. 4c; Tab. 2).

Tab. 1: Statistics of the ChRM directions for Cretaceous samples after different types of corrections. ΔD is the 95% confidence limit for declination calculated by a von Mises statistics (STEPHENS 1962), and ΔI is the 95% confidence limit for inclination calculated by a Fisherian statistics (MCFADDEN & REID 1982; CLARK 1983).

Type of correction	Declination	ΔD	Inclination	ΔI
Cretaceous samples with normal polarity (n= 106)				
Before bedding correction	259.4	5.6	38.9	2.8
After bedding correction	309.0	4.9	35.5	3.5
After bedding/rotational correction	330.9	4.0	35.5	3.5
After fold axis/bedding correction	307.6	3.5	32.6	4.9
Cretaceous samples with reversed polarity (n= 35)				
Before bedding correction	91.1	4.2	-25.0	4.5
After bedding correction	134.2	5.6	-40.4	3.9
After bedding/rotational correction	134.2	5.6	-40.4	3.9
After fold axis/bedding correction	144.7	4.7	-43.5	4.7

Tab. 2: Statistics of the ChRM directions after bedding correction and rotational correction (k = precision parameter; α_{95} = confidence limit)

Polarity	Number of samples	Declination	Inclination	k	α_{95}
Normal polarity	167	332.6	37.7	13.11	3.13
Reversed polarity	62	126.5	-42.4	10.09.	5.98

4.1.1 Magnetostratigraphy

The Cerbara section reveals five normal and five reversed polarity intervals (Fig. 5). The section starts with a long, clearly defined normal polarity zone which covers the first 7.22 m. Then a 25 cm thick zone with SE declination and an inclination of –24° was determined at 7.22 m, while the next 10.85 m show again normal polarity. A clear change from normal to reversed polarity occurs at 18.32 m. This reversed interval covers the uppermost part of the Cretaceous and 0.7 m of the Paleogene, and can be correlated via the C/P boundary with Chron 29R. Consistently, the two normal polarity zones in the Cretaceous part are identified as Chrons 30N and 31N. In the Palaeogene four reversed polarity zones and three normal polarity zones occur, spanning Chrons 29N to 26R. In the upper part of the section the position of the polarity changes cannot be exactly defined because some limestone beds did not show uniform indications for either normal or reversed polarity. This spans two intervals in the section of about 10 to 15 cm at the level of 26.32 m and 26.9 m. At the level of 28.3 m there occurs a bigger gap in the polarity sequence of about 35 cm. In these limestone beds no primary magnetization direction could be identified. The section ends in a reversed polarity zone.

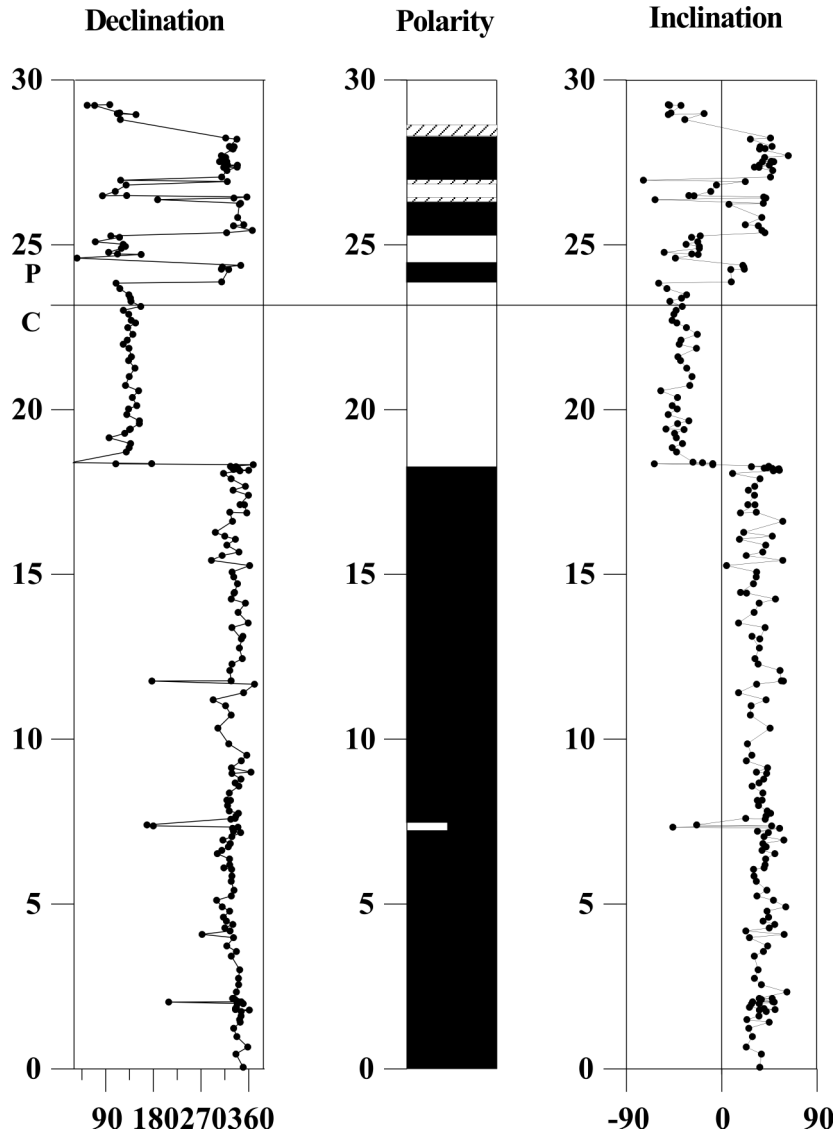

Fig. 5: Declination, inclination and polarity sequence of ChRM in the Cerbara section.

4.2. Stable Isotopes

4.2.1. Carbon isotopes

$\delta^{13}C$ data vary between 2.1‰ and 2.8‰ in the Cretaceous and from 1.3‰ to 2.2 ‰ in the Paleogene (Fig. 8). The first 2 m are characterised by a decrease of about 0.3 ‰. In the next 5 m $\delta^{13}C$ is relatively constant with values around 2.5 ‰. The following samples show some scatter, and at a level of 8 m the values increase again to 2.7 ‰. This

peak is followed by a continuous decrease up to meter 10 to 11. The next 3 m are characterised by an increase in $\delta^{13}C$. A significant feature of the $\delta^{13}C$ record in the Cerbara section is the abrupt decrease between adjacent samples at 14.25 m and 14.43 m. The upper part of the Cretaceous is again characterised by a relatively stable $\delta^{13}C$ record, with an increasing scatter at higher levels. The last Cretaceous samples show higher values of about 2.4 ‰. At the C/P boundary a sudden $\delta^{13}C$ depletion of 0.5‰ is discernable. In the Paleogene part of the Cerbara section the $\delta^{13}C$ data show a general trend toward lighter values from the C/P boundary onward. The lowest value is observable at 5.6 m above the C/P boundary. In the last 0.5 m of the section the trend towards lower values seems to stop.

4.2.2. Oxygen isotopes

$\delta^{18}O$ values vary more than the $\delta^{13}C$ data, i.e., from –2.1 ‰ up to –0.8 ‰ (Fig. 8). Starting at the bottom of the section a similar feature as in the $\delta^{13}C$ record can be seen: in the first meter there is a decrease in $\delta^{18}O$ of about 0.5 ‰. At 5 m another decrease by about 0.2‰ is observable. In the next 10 m $\delta^{18}O$ shows a trend to slightly heavier values, however, with a big scatter. This trend peaks at 14.25 m with a δ^{18} O value of –1.4 ‰. Corresponding to the decrease in $\delta^{13}C$ at about 14.3 m $\delta^{18}O$ decreases by 0.4‰ . Until just below the C/P boundary $\delta^{18}O$ values are around –2.0‰. The last three samples in the Cretaceous part of the section show slightly increasing values. This trend is going on in the Paleogene part where one peak was measured about 8 cm above the boundary with a value of –0.8 ‰, followed by a rapid decrease of about 0.6‰. A second peak of heavier values is at 1.8 m above the C/P boundary. This peak is again followed by lighter values of about –1.3 ‰. The next three samples show a continuous trend to lighter values, peaking at –2.0‰ at a level of 3 m above the boundary. This decreasing trend is succeeded by an opposite trend to heavier values in the following three samples with a highest $\delta^{18}O$ values of –1.0‰ at 3.3 m above the boundary. Then again the values decrease in the next four samples. Towards the end of the section the values seem to be relatively constant with some scatter.

Diagenetic overprint can alter primary isotope signals and complicate the interpretation of stable isotope curves. The presence of diagenesis can be tested by the correlation between carbon and oxygen isotopes: High correlations can often indicate the presence of diagenesis, but covariance can also derive from primary environmental conditions (CORFIELD 1991, MITCHELL et al 1997, STÜBEN et al. 2002). For the Cerbara section $\delta^{18}O$ and $\delta^{13}C$ values yield a correlation coefficient of $r = 0.67$ for the Cretaceous, and $r = 0.79$ for the Paleogene, giving evidence for isotope signals altered by diagenesis.

4.3. Biostratigraphy

The classification of the calcareous nannofossils is based on FARINACCI (1969), PERCH-NIELSEN (1985), AUBRY (1984), BOWN & YOUNG (1997), YOUNG & BOWN (1997a, 1997b) and BOWN (1998). Identification of species was made under a light microscope (LM) with 1000 x magnification. In the studied samples 16 taxa in the Cretaceous and 18 taxa in the Paleogene were recognized. Preservation of calcareous nannoplankton in

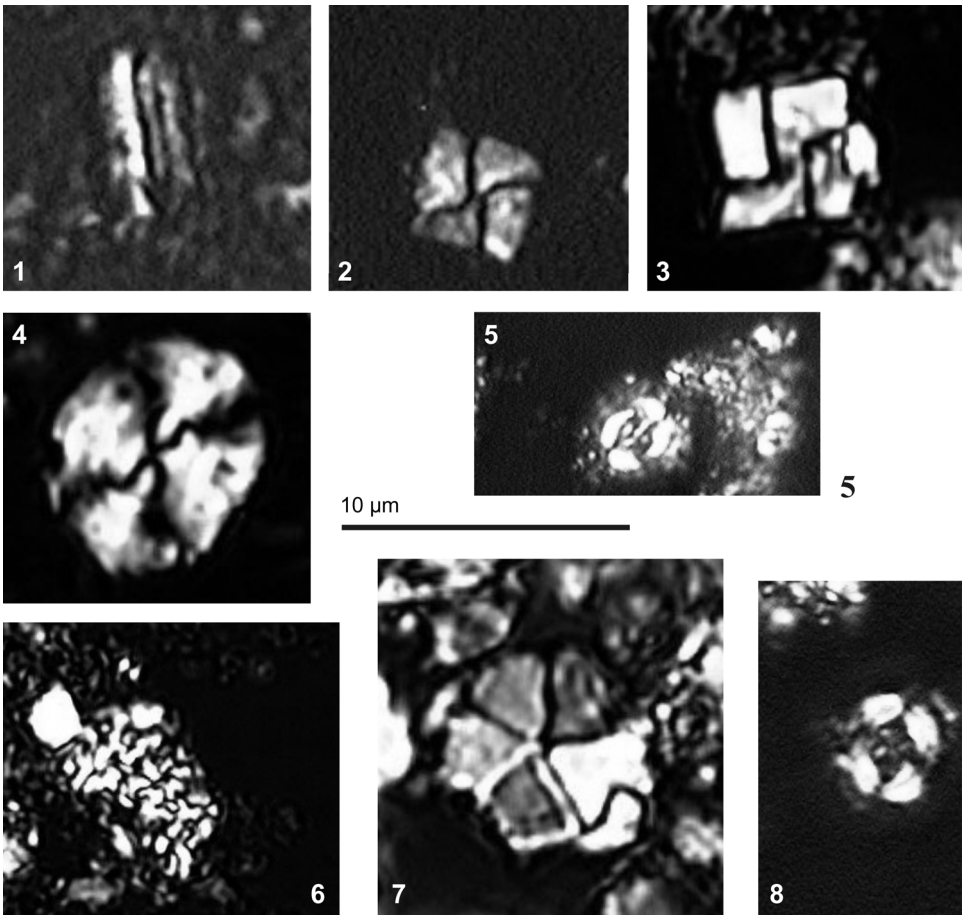

Fig. 6: LM images under crossed nicols of calcareous nannoplankton:

Cretaceous forms: 1 *Lithraphidites quadratus*; 2 *Micula praemurus*; 3 *Micula murus*; 4 *Watznaueria barnesae*.

Paleogene forms: 5 *Cruciplacolithus primus*; 6 *Thoracosphaera operculata;* 7 *Braarudosphaera bigelowii;* 8 *Chiasmolithus danicus*.

the samples was very poor due to recrystallisation and dissolution. In addition only a small number of forms was found in each sample, so that an evaluation of percental frequencies or relative abundances was not possible. Nevertheless, some marker species for calcareous nannoplankton zonations (Fig. 6) could be recognized in the samples. In the Cretaceous especially the marker species *Lithraphidites quadratus* (Fig. 6/1) and *Micula murus* (Fig. 6/3) for nannoplankton zones NC 22 and NC 23 were found. The lowest Paleogene samples of the Cerbara section are characterised by nearly monospecific occurrences of *Thoracosphaera operculata* (Fig. 6/6) and *Braarudosphaera bigelowii* (Fig. 6/7). This bloom is known from all Tethyan sections (GARTNER 1996). At a level of 1.8 m above the boundary *Thoracosphaera operculata* is still more abun-

dant than other forms, but the abundance of *Braarudosphaera bigelowii* decreases, while the abundance of Paleogene families like Coccolithaceae increases. The next 75 cm show typical Paleogene calcareous nannofossils but no zonal marker species were found. The occurrence of *Neochiastozygus modestus* at 25.41 m is a hint for calcareous nannoplankton zone NP3 (MARTINI 1971)/ CP2 (OKADA & BUKRY 1980). *Chiasmolithus danicus* (Fig. 6/8) at a level of 2.8 m above the boundary indicates calcareous nannoplankton zone NP3/CP2. In some higher samples (4.1 m above the boundary) also some calcareous nannoplankton forms indicative for zone NP4 (*Neochiastozygus saepes, Ellipsolithus macellus*) seem to be present.

5. Discussion and Interpretation

5.1. Cretaceous Bio- and Magnetostratigraphy

In the GPTS the C/P boundary is dated at 65 Ma and lies within magnetostratigraphic zone 29R, but the position of the C/P-boundary event within magnetochron 29R is not exactly defined (BERGGREN et al. 1995). In the C/P boundary section of Bjala the absolute geological age of magnetochron 29R was estimated by correlation with Mylankovitch cycles (PREISINGER et al. 2000, 2001).

Interpretation of the magnetostratigraphic pattern of Cerbara and correlation to the GPTS is based on the identification of Chron 29R. One definitive marker in the Cerbara section is the 2-3 cm thick Cretaceous-Paleogene boundary clay showing the typical iridium anomaly (MONTANARI 1991) lying in a reversed magnetozone.

The Cretaceous pattern of reversed and normal polarity zones in Cerbara fits very well with the nearby section of the Bottaccione Gorge (ROGGENTHEN & NAPOLEONE 1977, LOWRIE & ALVAREZ 1977) and other Umbrian sections (Fig. 7): The change from Chron 30N to 29R in Cerbara is 4.9 m below the C/P-boundary, and 4.6 m in Bottaccione. The identified short reversed magnetozone at 7.22 m in Cerbara can be correlated with the small reversed polarity zone 31R in Bottaccione.

The Paleogene part displays a more complex pattern as the chrons do not correlate as well as in the Cretaceous part (Fig. 7). Assuming a complete record in the Cerbara section, the three normal polarity zones in the Paleogene are primarily identified as chrons 29N, 28N, and 27N. The completeness of the section is estimated by its biostratigraphical record. *Lithraphidites quadratus* was recognized at the base of the section, correlating the base to nannoplankton zone NC22 (zonation after ROTH 1978) (Fig. 8). The first occurrence of *Micula murus* at 11.19 m indicates zone NC23 (*Micula murus* zone). *Micula prinsii*, typical for the uppermost Maastrichtian was not found in any sample. The lack of *Micula prinsii* does not conclusively mean that the uppermost Cretaceous part is missing. In nearly all Cretaceous samples a relatively high abundance of *Watznaueria barnesae* (Fig. 6/4) was evident. As this form is the most common one in poorly preserved assemblages, the lack of *Micula prinsii* can result from its poor preservation because of being susceptible to dissolution (GARDIN 2002).

The lowest Paleogene samples are dominated by *Thoracosphaera operculata* and *Braarudosphaera bigelowii*. The dominance of *Thoracosphaera operculata* and *Braarudosphaera bigelowii* is known from many C/P boundary sites (GARTNER 1996).

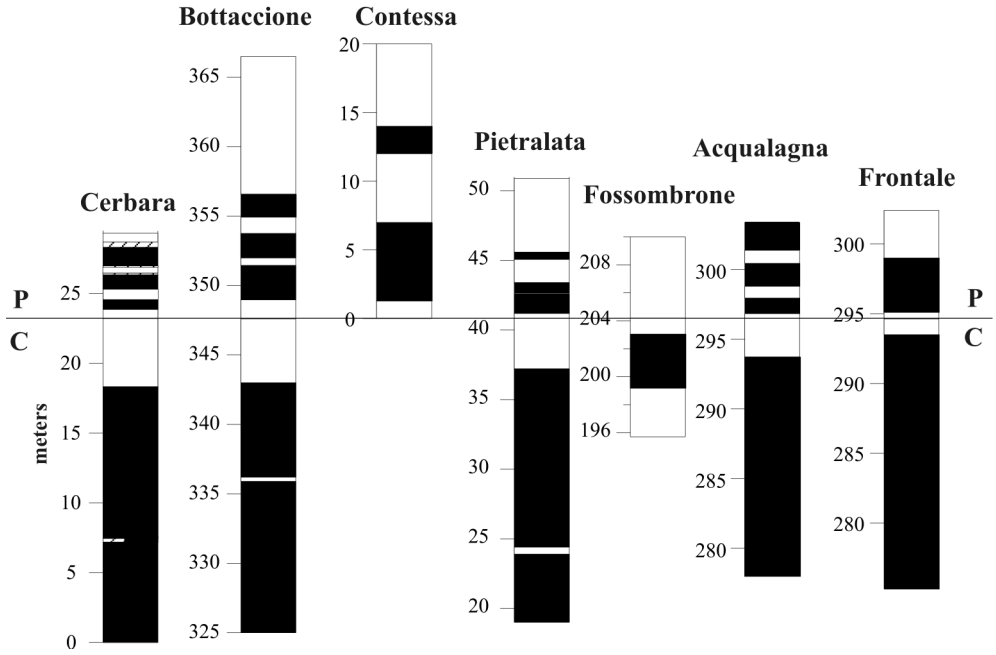

Fig. 7: Correlation of the Cerbara section with other Umbrian sections (Bottacchione after ROGGENTHEN & NAPOLEONE 1977, LOWRIE & ALVAREZ 1977; Contessa after LOWRIE et al. 1982; Pietralata after ALVAREZ & LOWRIE 1984; Fossombrone, Acqualagna, Frontale after CHAN et al. 1985).

A detailed biostratigraphic zonation for the first 2 m of the Paleogene is missing. At 25.45 m *Neochiastozygus modestus*, correlated with zone NP3 (zonation after MARTINI 1971), was found. The first occurence of *Chiasmolithus danicus*, the marker for the NP3 zone, was at 26 m. In spite of the poor preservation *Neochiastozygus saepes* at 27.4 m and *Ellipsolithus macellus* at 28.9 m were most probably identified, indicating zone NP4 for the uppermost part of the section. The biostratigraphic results of the Cretaceous part correlate well with the magnetostratigraphy. The base of the section is characterised by normal polarity and the occurrence of *Lithraphidites quadratus*. In the Bottaccione section *Lithraphidites quadratus* appears just above the base of subchron 31N (MONECHI & THIERSTEIN 1985). In three of the South Atlantic Sites (POORE et al. 1983, MANIVIT 1984) the first occurence of *Lithraphidites quadratus* was observed in Subchron 31N and in Subchron 30N at DSDP Site 530A. The first occurrence of *Micula murus*, which characterises the uppermost identified biostratigraphic zone in the Cerbara section, is at level 11.19 m. This coincides with the lower part of Chron 30N. *Micula murus* appears near the base of 30N in the Bottaccione section and at DSDP Site 524, while it appears in mid-Subchron C30N at DSDP Sites 525A and 527 (MONECHI & THIERSTEIN 1985). The interpretation of the normal magnetozone at the base of the Cerbara section as part of Chron 31N, the very short reversed zone as hint for Chron 30R, and the following normal zone as Chron 30N, are clearly supported by the biostratigraphic results. The identification of Chron 29R is unambiguous by the presence of the C/P boundary lying in this reversed chron.

The view that many FAD´s and LAD´s of Cenozoic calcareous nannofossil species are unreliable because of preservational problems or latitudinal diachrony is still in discussion. Most of the discrepancies in magnetostratigraphic correlations between different sections can be related to undeciphered inconformities in the stratigraphic record, and do not reflect diachrony, although diachrony can certainly occur (BERGGREN et al. 1995).

5.2. Paleogene Bio- and Magnetostratigraphy

A recent nannoplankton biostratigraphic and magnetostratigraphic correlation is based on DSDP Site 384 (NW Atlantic Ocean), which is essentially the same as established by MONECHI & THIERSTEIN (1985) in the sections near Gubbio (BERGGREN et al. 2000): the FAD of *Chiasmolithus danicus* lies in late Chron 29N, and the FAD of *Ellipsolithus macellus* in earliest Chron 27R. Compared to the correlation of BERGGREN et al. (1995), the FAD of *Chiasmolithus danicus* has been shifted from Chron 28R or 28N (depending on which DSDP Site the correlation is based) to Chron 29N in DSDP Site 384.

The lowest *Chiasmolithus danicus* (inclusive of *Cruciplacolithus edwardsii*) occurs in the first normal subchron above the C/P boundary in all Tethyan, Atlantic and Pacific sections, and the lowest occurrence of *Ellipsolithus macellus* is observed in Subchron C27R in the Bottaccione and Contessa sections (MONECHI & THIERSTEIN 1985). At DSDP Sites 525A and 527 it is observed in Chron C27R (MANIVIT 1984), while at DSDP Sites 524, 577 and 577A the first occurrence of *Ellipsolithus macellus* is dated younger in the Subchron C26R (POORE et al. 1983, MONECHI et al. 1985).

The lack of other forms than *Thoracosphaera operculata* and *Braarudosphaera bigelowii* in the lowest Paleogene samples hinders the establishment of a nannoplankton zone. Generally, the bloom of these two species is a short-dated event directly above the C/P boundary (GARTNER 1996). At 26.0 m the occurrence of *Chiasmolithus danicus* defines zone NP3, but the presence of *Neochiastozygus modestus* about 50 cm below seems to indicate the lower boundary of the zone at 2.2 m above the C/P boundary. This level is within the lower part of normal polarity magnetozone 28N. The higher part of NP3 correlates with magnetozone 27R. 4.2 m above the C/P boundary nannoplankton species representative for NP4 were most probably recognized, especially *Neochiastozgyus saepes* and *Ellipsolithus macellus.* Based on this moderately reliable identification of appearances, the boundary of zone NP4 correlates with the lower part of magnetozone 27N. A really reliable determination of appearance levels could not be established due to the poor preservation and low abundances, but the presence of nannoplankton zones NP3 and NP4 in the upper part of the Cerbara section seems to be evident. Compared to the magnetobiostratigraphical correlations of BERGGREN et al. (1995) and BERGGREN et al. (2000), the correlation of the first occurrences in the Paleogene of the Cerbara section is time delayed, and the dominance of *Thoracosphaera operculata* and *Braarudosphaera bigelowii* lasts too long. The zonal marker forms occur systematically later.

5.3. Isotope Stratigraphy

Though diagenetic overprint of the isotope signal must be assumed, isotopic trends reflect the most prominent known isotopic changes at the C/P boundary (Fig. 8). $\delta^{13}C$ values decrease clearly at the boundary. $\delta^{13}C$ data indicate relatively stable bioproductivity

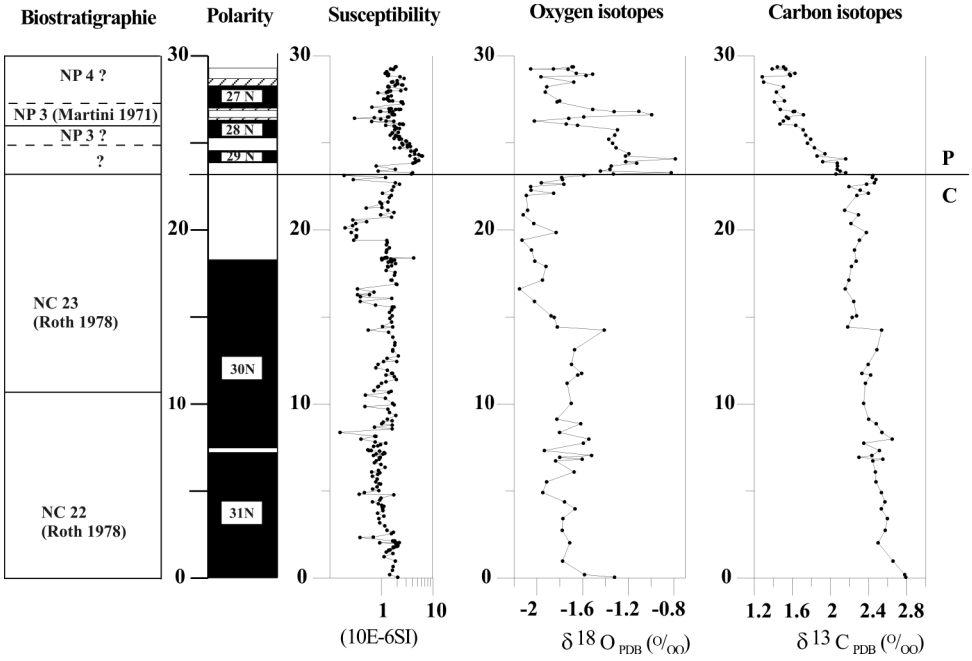

Fig. 8: Correlation of magnetostratigraphy, biostratigraphy and stable isotope stratigraphy for the Cerbara section.

during the late Maastrichtian (STÜBEN et al. 2002). A negative shift of $\delta^{13}C$ in bulk samples, combined with a reduced $CaCO_3$ accumulation and correlated faunal changes, have been recognized globally in C/P boundary sections. Benthic $\delta^{13}C$ records in deep water environments do not show this decrease, suggesting that the decrease was restricted to surface waters which can be seen as a result of a reduction of ocean primary productivity (KELLER & LINDINGER 1989, THIERSTEIN & BERGER 1978, HSÜ et al. 1982, PERCH-NIELSEN et al. 1982, ARTHUR et al. 1987, D`HONDT 1998, STÜBEN et al. 2002).

In contrast to the negative $\delta^{13}C$ excursion $\delta^{18}O$ shows an increasing trend across the boundary. At the C/P boundary a trend towards a positive excursion of $\delta^{18}O$ values in benthic foraminifera, indicative for colder water temperatures, was observed at DSDP Site 398 (ARTHUR et al. 1979), Site 356 (BOERSMA 1984) and Site 577 (ZACHOS et al. 1985), El Kef (KELLER & LINDINGER 1989) and Elles (STÜBEN et al. 2002). In contrast, fine fraction $\delta^{18}O$ values show a decrease of about 2 ‰ in El Kef/Tunisia (KELLER & LINDINGER 1989), Negev/Israel (Magaritz et al. 1985), Caravaca/Spain and Biarritz/France (ROMEIN & SMIT 1981), Lattengebirge/Austria (PERCH-NIELSEN et al. 1982), South Atlantic Site 524 (HSÜ et al. 1982), Site 384 and 356 (BOERSMA et al. 1979) and Braggs/Alabama (JONES et al. 1987). These conflicting benthic and fine fraction $\delta^{18}O$ ratios in the Tunisian sections and many deep-sea sections can be interpreted as reflecting diagenetic and compositional effects (KELLER & LINDINGER 1989).

6. Conclusion

1) Thermal treatment of the samples led to a sucessful demagnetization and ChRM directions yielded 5 normal and 5 reversed polarity zones. Interpretation of the magnetozones leads to identification of magnetozones 31N to 29R for the Cretaceous and 29R to 26R for the Paleogene.

2) Though calcareous nannoplankton is poorly preserved and less abundant, species indicative for Cretaceous nannoplankton zones NC22 and NC23 and Paleogene nannoplankton zone NP3 and NP4 were recognized. The lowest Paleogene samples are characterised by a nearly monospecific occurrence of *Thoracosphaera operculata* and *Braarudosphaera bigelowii*.

3) The base of nannoplankton NC 23 is correlated with the lower part of magnetozone 30N. In the Paleogene part, the base of NP3 is within the lower part of normal polarity magnetozone 28N. The higher part of NP3 correlates with magnetozone 27R. Based on moderatly reliable identifications of occurences of *Neochiastozgyus saepes* and *Ellipsolithus macellus*, the boundary of zone NP4 correlates with the lower part of magnetozone 27N.

4) Diagentic overprinting of the oxygen and carbon isotopes can not be ruled out but nevertheless stable isotopes show characteristic patterns across the Cretaceous-Paleogene boundary: $\delta^{13}C$ values decrease by about 0.5‰, while $\delta^{18}O$ values increase by about 1.0‰.

5) For the Cerbara section magnetostratigraphy provided the most reliable results which are supported by biostratigraphical data of calcareous nannoplankton. Biostratigraphic results do not lead to a higher resolution in time, because of the observed delay and deviation from the normal succession of nannofossil events in other Paleogene sections which can be related to dissolution and recrystallisation. Stable isotope stratigraphy did not yield a better time resolution because of diagenetic overprinting.

Acknowledgements

This work was financially supported by the Austrian Science Fund (FWF P 12643 GEO; project leader A. Preisinger). The opportunities to do my research at the Paleomagnetic Laboratory in Gams (Geophysical Institute, University of Leoben) under supervision of Robert Scholger are gratefully acknowledged. I wish to express my gratitude to Werner Piller (Institute for Geology and Paleontology, University of Graz) and Hermann J. Mauritsch (Institute of Geophysics, University of Leoben) for valuable dicussions and support during this study. I sincerely thank Katharina von Salis for introducing me into the work with calcareous nannofossils.

References

ALVAREZ, L.W., ALVAREZ, W., ASARO, F. & MICHEL, H.V. (1980): Extraterrestrial cause for the Cretaceous-Tertiary extinction. – Science, **208**: 1095-1108. – Washington D.C.

ALVAREZ, W. & LOWRIE, W. (1978): Upper Cretaceous paleomagnetic stratigraphy at Moria (Umbrian Apennines, Italy): Verification of the Gubbio section. – Geophys. J. R. Astr. Soc., **55**: 1-17. – Oxford.

—— & LOWRIE, W. (1984): Magnetic stratigraphy applied to synsedimentary slumps, turbidites and basin analysis: The Scaglia limestone at Furlo (Italy). – Geol. Soc. Am. Bull., **95**: 324-336. – Boulder.

—— , COLACICCHI, R. & MONTANARI, A. (1985): Synsedimentary slides and bedding formation in Apennines pelagic limestones. – J. Sed. Petrol., **55**: 720-734. – Tulsa.

—— , ARTHUR, M.A., FISCHER, A.G., LOWRIE, W., NAPOLEONE, G., PREMOLI SILVA, I. & ROGGENTHEN, W.M. (1977): Upper Cretaceous-Paleocene magnetic stratigraphy at Gubbio, Italy V. Type section for the late Cretaceous-Paleogene geomagnetic reversal time scale. – Geol. Soc. Am. Bull., **88**: 383-389. – Boulder.

ARTHUR, M.A. & FISCHER, A.G. (1977): Upper Cretaceous-Paleocene magnetic stratigraphy at Gubbio, Italy. I. Lithostratigraphy and sedimentology. – Geol. Soc. Am. Bull., **88**: 367-371. – Boulder.

—— , SCHOLLE, P.A. & HASSON, P. (1979): Stable isotopes of oxygen and carbon in carbonates from Sites 398 and 116 of the Deep Sea Drilling Project. **–** In: Initial Reports of the Deep Sea Drilling Project, **47**: 477-492. **–** Washington, D.C. (U.S. Government Printing Office).

—— , ZACHOS, J.C. & JONES, D.S. (1987): Primary productivity and the Cretaceous/Tertiary boundary event in the oceans. – Cretaceous Res., **8**: 43-45. – London.

AUBRY, M.P. (1984 et seq.): Handbook of Cenozoic calcareous nannoplankton, Book 1-4. – New York (Micropaleontology Press, American Museum of Natural History).

BALDANZA, A., COLACICCHI, R. & PARISI, G. (1982): Controllo tettonico sulla deposizione dei livelli detritici della Scaglia cretaciico-terziaria (Umbria oriental). – Rend. Soc. Geol. It., **5**: 11-14. – Rome.

BERGGREN, W.A., AUBRY, M.-P., VAN FOSSEN, M., KENT, D.V., NORRIS, R.D. & QUILLEVERE, F. (2000): Integrated Paleocene calcareous plankton magnetobiochronology and stable isotope stratigraphy: DSDP Site 384 (NW Atlantic Ocean). **–** Palaeogeogr. Palaeoclimatol. Palaeoecol., **159**: 1-51. – Amsterdam.

—— , KENT, D.V., SWISHER, C.C. III & AUBRY, M.-P. (1995): A revised Cenozoic geochronology and chronostratigraphy. **–** In: BERGGREN, W.A., KENT, D.V., AUBRY, M.-P. & HARDENBOL, J. (eds.): Chronology, time scales and global stratigraphic correlation. **–** SEPM Special Publication **54**: 129-212. – Tulsa.

BOERSMA, A. (1984): Comparison through Paleocene paleotemperature and carbon isotope sequence and the Cretaceous/Tertiary boundary in the Atlantic Ocean. **–** In: BERGGREN, W.A. & VAN COUVERING, J.A. (eds.): Catastrophisms in Earth History, The New Uniformitarism, 147-178. **–** Princeton, N.J. (Princeton University Press).

—— , SHACKLETON, N.J., HALL, M. & GIVEN, Q. (1979): Carbon and Oxygen isotope records at DSDP Site 383 (North Atlantic) and some Paleocene paleotemperatures and carbon isotope variations in the Atlantic Ocean. **–** In: Initial Reports of the Deep Sea Drilling Project, **43**: 695-717. **–** Washington, D.C. (U.S. Government Printing Office).

BOWN, P.R. (1998): Calcareous Nannofossil Biostratigraphy. – 314 pp. – London (Chapmann & Hall).

—— & YOUNG, J.R. (1997): Mesozoic calcareous nannoplankton classification. – Journal of Nannoplankton Research, **19**: 21-36. – The Hague.

CHAN, L.S., MONTANARI, A. & ALVAREZ, W. (1985): Magnetic stratigraphy of the Scaglia Rossa: Implications for syndepositional tectonics of the Umbria-Marche basin. – Riv. It. Paleont. Strat., **91**/2: 219-258. – Milan.

CHANNEL, J.E.T., D´ARGENIO, B. & HOWARTH, F. (1979): Adria, the African Promontory in Mesozoic Mediterranean paleogeography. – Earth Sci. Review, **15**: 213-292. – Amsterdam.

CLARK, R.M. (1983): Estimations of parameters in the marginal Fisher distribution. – Austral. J. Statist., **25**: 227-237. – Canberra.

CORFIELD, R.M., CARTLIDGE, J.E., PREMOLI SILVA, I. & HOUSLEY, R.A. (1991): Oxygen and carbon isotope stratigraphy of the Paleogene and Cretaceous limestones in the Bottaccione Gorge and the Contessa Highway sections, Umbria, Italy. – Terra Nova, **3**: 414-422. – Oxford.

D´HONDT, S. (1998): Isotopic proxies for ecological collapse and recovery from mass extinction. – The Paleontological Society Papers, **4**: 179-211. – Lawrence.

FARINACCI, A. (1969 et seq.): Catalogue of calcareous nannofossils. 13 vols. **–** Edizioni Tecnoscienza. **–** Roma.

GARDIN, S. (2002): Late Maastrichtian to early Danian calcareous nannofossils at Elles (North West Tunisia). A tale of one million years across the K-T boundary. – Palaeogeogr. Palaeoclimatol. Palaeoecol., **178**/3-4: 211-231. – Amsterdam.

GARTNER, S. (1996): Calcareous Nannofossils at the Cretaceous-Tertiary Boundary. – In: MACLEOD, N. & KELLER, G. (eds.): Cretaceous-Tertiary Mass Extinctions: Biotic and Environmental Changes, 27-42. – New York (W.W. Norton & Company).

HILDEBRAND, A.R., PENFIELD, G.T., KRING, D.A., PILKINGTON, M., CAMARGO, Z.A., JACOBSEN, S. & BOYNTON, W.V. (1991): A possible Cretaceous-Tertiary boundary impact crater on the Yucatan peninsula, Mexico. **–** Geology, **19**: 867-871. – Boulder.

HSÜ, K.J., HE, Q., MCKENZIE, J.A., WEISSERT, H., PERCH-NIELSEN, K., OBERHÄNSLI, H., KELTS, K., LABRECQUE, J., TAUXE, L., KRAHENBUHL, U., PERCIVAL, S.F., WRIGHT, R., KARPOFF, A.M., PETERSEN, N., TUCKER, P., POORE, R.Z., GOMBOS, A.M., PISCIOTTO, K.A., CARMAN, M.F. & SCHREIBER, E. (1982): Mass mortality and its environmental and evolutionary consequences. – Science, **216**: 249-256. – Washington D.C.

JONES, D.S., MUELLER, P.A., BRYAN, J.R., DOBSON, J.P., CHANNEL, J.E.T., ZACHOS, J.C. & ARTHUR, M.A. (1987): Biotic, geochemical and paleomagnetic changes across the Cretaceous/Tertiary boundary at Braggs, Alabama. – Geology, **15**: 311-315. – Boulder.

KELLER, G. & LINDINGER, M. (1989): Stable isotope, TOC and $CaCO_3$ record across the Cretaceous/Tertiary boundary at El Kef, Tunisia. – Palaeogeogr. Palaeoclimatol. Palaeoecol., **73**/3-4: 243-265. – Amsterdam.

KROOPNICK, P. (1980): Isotopic fractionations during oxygen consumption and carbonate dissolution within the North Atlantic Deep Water. – Earth Planet. Sci. Lett., **49**: 485-498. – Amsterdam.

KYTE, F.T. (1998): A meteorite from the Cretaceous/Tertiary boundary. – Nature, **396**: 237-239. – London.

LATAL, C., SCHOLGER, R. & PREISINGER, A. (2000): Paleomagnetic Investigations Imply Rotations Within The Cretaceous-Tertiary Transitions Section at Cerbara (Italy). – Phys. Chem. Earth (A), **25**/5: 499-503. – Oxford.

LOWRIE, W. (1990): Identification of ferromagnetic minerals in a rock by coercivity and unblocking temperature properties. – Geophys. Res. Lett., **17**: 159-162. – Washington D.C.

—— & ALVAREZ, W. (1977): Upper Cretaceous-Paleocene magnetic stratigraphy at Gubbio, Italy. III. Upper Cretaceous magnetic stratigraphy. **–** Geol. Soc. Am. Bull., **88**: 374-377. – Boulder.

—— , ALVAREZ, W., NAPOLEONE, G., PERCH-NIELSEN, K., PREMOLI SILVA, I. & TOURMARKINE, M. (1982): Paleogene magnetic stratigraphy in Umbrian pelagic carbonate rocks: The Contessa sections, Gubbio. **–** Geol. Soc. Am. Bull., **93**: 414-432. – Boulder.

LUTERBACHER, H.P. & PREMOLI SILVA, I. (1962): Note preliminaire sur une revision du profil de Gubbio, Italie. – Riv. It. Paleont. Strat., **68**: 253-288. – Milan.

MAGARITZ, M., MOSHKOVITZ, S., BENJAMINI, C., HANSEN, H.J., KAKANSSON, E. & RASMUSSEN, S. (1985): Carbon isotope bio- and magnetostratigraphy across the Cretaceous-Tertiary boundary in the Zin Valley, Negev, Israel. – Newsl. Stratigr., **15**/2: 100-102. – Stuttgart.

MANIVIT, H. (1984): Paleogene and Upper Cretaceous calcareous nannofossils from Deep Sea Drilling Project Leg 74. – Initial Reports of Deep Sea Drilling Project, **74**: 475-499. – Washington D.C. (U.S. Government Printing Office).

MARTINI, E. (1971): Standard Tertiary and Quaternary calcareous nannoplankton zonation. – In: FARINACCI, A. (ed.): Proceedings of the Second Planktonic Conference, Roma 1970. – Edizioni Tecnoscienza, **2**: 739-785. – Roma.

MACLEOD, N. (1996): K/T redux. – Paleobiology, **22**/3: 311-317. – Lancaster.

MCFADDEN, P.L. & REID, A.B. (1982): Analyses of paleomagnetic inclination data. – Geophys. J. R. Astr. Soc., **69**: 307-319. – London.

MITCHELL, S.F., BALL, J.D., CROWLEY, S.F., MARSHALL, J.D., PAUL, C.R.C., VELTKAMP, C.J. & SAMIR, A. (1997): Isotope data from cretaceous chalks and foraminifera: Environmental or diagenetic signals? – Geology, **25**: 691-694. – Boulder.

MONECHI, S. (1977): Upper Cretaceous and Early Tertiary Nannoplankton from the Scaglia Umbra Formation (Gubbio, Italy). – Riv. Ital. Paleont. Strat., **83**: 759-802. – Milan.

—— & RADRIZZANI, C.P. (1975): Nannoplankton from Scaglia Umbra Formation (Gubbio) at Cretaceous-Tertiary Boundary. – Riv. Ital. Paleont., **81**: 31-44. – Milan.

—— & THIERSTEIN, H. (1985): Late Cretaceous-Eocene nannofossil and magnetostratigraphic correlations near Gubbio, Italy. – Marine Micropaleontology, **9**: 419-440. – Amsterdam.

—— , BLEIL, U. & BACKMAN, J. (1985): Magnetobiochronology of Late Cretaceous-Paleogene and Late Cenozoic pelagic sedimentary sequences from the NW-Pacific (DSDP Leg 86, Site 577). – In: Initial Reports of the Deep Sea Drilling Project, **25**: 579-634. – Washington, D.C. (U.S. Government Printing Office).

MONTANARI, A. (1991): Authigenesis of impact spheroids in the K/T boundary clay from Italy: New constraints for high-resolution stratigraphy of terminal Cretaceous events. – J. Sed. Petrol., **61**/3: 315-339. – Tulsa.

—— & KOEBERL, C. (2000): Impact Stratigraphy – The Italian Record. – Lecture Notes in Earth Sciences. – 364 pp. – Berlin (Springer Verlag).

—— , CHAN, L.S. & ALVAREZ, W. (1989): Synsedimentary tectonic in the Late Cretaceous-Early Tertiary pelagic basin of the Northern Apennines. – In: CREVELLO, P.D., WILSON, J.L., SARG, J.F. & READ, J.F. (eds): Controls on Carbonate Platform and Basin Development. – SEPM Special Publication, **44**: 379-399. – Tulsa.

OKADA, H. & BUKRY, D. (1980): Supplementary modification and introduction of code numbers to the low-latitude coccolith biostratigraphic zonation. – Marine Micropaleontology, **5**: 321-325. – Amsterdam.

PERCH-NIELSEN, K., MCKENZIE, J. & HE, Q. (1982): Biostratigraphy and isotope stratigraphy and the „catastrophic" extinction of calcareous nannoplankton at the Cretaceous/Tertiary boundary. – In: SILVER, L.T. & SCHULZ, H.P. (eds.): Geological implications of impacts of large asteroids and comets on the Earth. – Geol. Soc. Am. Mem., **190**: 353-371. – Boulder.

—— (1985): Mesozoic calcareous nannofossils. – In: BOLLI, H.M., SAUNDERS, J.B. & PERCH-NIELSEN, K. (eds): Plankton Stratigraphy, 427-554. – Cambridge (Cambridge University Press).

POORE, R.Z., TAUXE, L., PERCIVAL JR., S.F., LABREQUE, J.L., WRIGHT, R., PETERSEN, N.P., SMITH, C.S., TUCKER, P. & HSU, K.J. (1983): Late Cretaceous-Cenozoic magnetostratigraphic and biostratigraphic correlation of the South Atlantic Ocean: DSDP Leg 73. – Palaeogeogr. Palaeoclimatol. Palaeoecol., **42**: 127-149. – Amsterdam.

POPE, K.O., OCAMPO, A.C. & DULLER, C.E. (1991): Mexican site for the K/T Crater? **–** Nature, **351**: 105. – London.

PREISINGER, A., ASLANIAN, S., BRANDSTAETTER, F., GRASS, F., STRADNER, H. & SUMMESBERGER, H. (2000): Cretaceous/Tertiary (K/T) profile, rhythmic deposition and geomagnetic reversals of marine sediments near Bjala, Bulgaria. – LPI Contribution, Report **1053**: 168. **–** Lunar and Planetary Institute, Houston, TX.

—— , ASLANIAN, S., BRANDSTAETTER, F. & GRASS, F. (2001): Rhythmic change of the intensity of Earth's magnetic field and fall of cosmic dust throughout geological time. – Meteoritics & Planetary Science, **36**/9: 168-169. **–** Fayetteville, AR. (Meteoritical Society).

PREMOLI SILVA, I. (1977): Upper Cretaceous-Paleocene magnetic stratigraphy at Gubbio, Italy. – II: Biostratigraphy. – Geol. Soc. Am. Bull., **88**: 371-374. – Boulder.

—— & SLITER, W.V. (1995): Cretaceous planktonic foraminiferal biostratigraphy and evolutionary trends from the Bottaccione section, Gubbio, Italy. – Palaeontographia Italica, **82**: 1-26. – Pisa.

RAMPINO, M.R. & HAGGERTY, B.M. (1996): Impact crisis and mass extinctions: A working hypothesis. In: RYDER, G., FASTOVSKY, D. & GARTNER, S. (eds.): The Cretaceous-Tertiary Event and Other Catastrophes in Earth History. – Geol. Soc. Am., Special Paper **307**: 11-30. – Boulder.

REMANE, J. & ADATTE, T. (eds) (2002): Cretaceous-Paleogene Transition in Tunisia, May 1998. – Palaeogeogr. Palaeoclimatol. Palaeoecol., **178**. Amsterdam.

ROGGENTHEN, W.M. & NAPOLEONE, G. (1977): Upper Cretaceous-Paleocene magnetic stratigraphy at Gubbio, Italy – IV: Upper Maastrichtian-Paleocene magnetic stratigraphy. – Geol. Soc. Am. Bull., **88**: 378-382. – Boulder.

ROMEIN, A.J.T. & SMIT, J. (1981): Carbon-oxygen stable isotope stratigraphy of the Cretaceous/Tertiary boundary interval. Data from the Biarritz section, SW France. – Geol. Mijnbouw, **6**/4: 541-544. – Amsterdam.

ROTH, P.H. (1978): Cretaceous nannoplankton biostratigraphy and oceanography of the northwestern Atlantic Ocean. – In: Initial Reports of the Deep Sea Drilling Project, **44**: 731-759. – Washington, D.C. (U.S. Government Printing Office).

SCHOLLE, P.A. & ARTHUR, M.A. (1980): Carbon isotope fluctuation in Cretaceous pelagic limestone: potential stratigraphic and petroleum exploration tool. – Bull. Am. Ass. Petrol. Geol., **64**/1: 67-87. – Tulsa.

SOFFEL, H.C. (1991): Paläomagentismus und Archäomagnetismus. – pp. 276. – Berlin (Springer Verlag).

STEPHENS, M.A. (1962): Exact and approximate test for directions I. – Biometrika, **49**: 463-477. – London.

STÜBEN, D., KRAMAR, U., BERNER, Z., SINNESBECK, W., KELLER, G. & ADATTE, T. (2002): Trace elements, stable isotopes, and clay mineralogy of the Elles II K-T boundary section in Tunisia: indications for sea level fluctuations and primary productivity. – Palaeogeogr. Palaeoclimatol. Palaeoecol., **178**: 321-345. Amsterdam.

THIERSTEIN, H.R. & BERGER, W.H. (1978): Injection events in oceanic history. – Nature, **276**: 461-466. – London.

WILLIAMS, D.F., SOMMER, M.A. & BENDER, M.L. (1977): Carbon isotopic composition of recent planktonic foraminifera of the Indian Ocean. – Earth Planet. Sci. Lett., **36**: 391-403. – Amsterdam.

YOUNG, J.R. & BOWN, P.R. (1997a): Higher classification of nannoplankton. – Journal of Nannoplankton Research, **19**: 15-20. – The Hague.

—— , BOWN, P.R. (1997b): Cenozoic calcareous nannoplankton classification. – Journal of Nannoplankton Research, **19**: 36-47. – The Hague.

ZACHOS, J.C. & ARTHUR, M.A. (1986): Paleoceanography of the Cretaceous/Tertiary boundary event: Inferences from stable isotopic and other data. – Paleoceanography, **1**: 5-26. – Washington D.C.

—— , ARTHUR, M.A., THUNELL, R.C., WILLIAMS, D.F. & TAPPA, E.T. (1985): Stable isotope and trace element geochemistry of carbonate sediments across the Cretaceous/Tertiary boundary at DSDP Hole 577, Leg 86. – In: Initial Reports of the Deep Sea Drilling Project, **86**: 513-532. – Washington, D.C. (U.S. Government Printing Office).